β-decay of odd-*A* ^{57}Ti and ^{59}V

S. N. Liddick,[1,2] P. F. Mantica,[1,2] R. Broda,[3] B. A. Brown,[1,4] M. P. Carpenter,[5] A. D. Davies,[1,4] B. Fornal,[3]
M. Horoi,[6] R. V. F. Janssens,[5] A. C. Morton,[1] W. F. Mueller,[1] J. Pavan,[7] H. Schatz,[1,4]
A. Stolz,[1] S. L. Tabor,[7] B. E. Tomlin,[1,2] and M. Wiedeking[7]

[1]*National Superconducting Cyclotron Laboratory, Michigan State University, East Lansing, Michigan 48824, USA*
[2]*Department of Chemistry, Michigan State University, East Lansing, Michigan 48824, USA*
[3]*Niewodniczanski Institute of Nuclear Physics, PL-31342, Cracow, Poland*
[4]*Department of Physics and Astronomy, Michigan State University, East Lansing, Michigan 48824, USA*
[5]*Physics Division, Argonne National Laboratory, Argonne, Illinois 60439, USA*
[6]*Department of Physics, Central Michigan University, Mount Pleasant, Michigan 48859, USA*
[7]*Department of Physics, Florida State University, Tallahassee, Florida 32306, USA*

The β-decay of odd-*A*, neutron-rich ^{57}Ti and ^{59}V are studied. More precise β-decay half-lives of 98 ± 5 and
97 ± 2 ms are deduced for ^{57}Ti and ^{59}V, respectively. In addition, β-delayed γ-ray spectroscopy is used to deduce
β-decay branching ratios and establish the low-energy-level structures of the daughter nuclides. The new data for
levels in ^{57}V and ^{59}Cr are compared with the results of shell-model calculations completed in the full *pf* model
space. Both ^{57}V and ^{59}Cr show evidence of modest oblate deformation near the ground state.

I. INTRODUCTION

The systematic behavior of the low-energy structures of neutron-rich nuclides in the vicinity of doubly magic ^{48}Ca has revealed a strong interplay between the proton and the neutron orbitals near the Fermi surface. The monopole migration of the $\nu f_{5/2}$ orbital with the changing occupancy of the $\pi f_{7/2}$ orbital produces a significant subshell gap at $N = 32$ for the even-even $_{24}$Cr [1,2], $_{22}$Ti [3], and $_{20}$Ca [4] isotopes. Shell-model results obtained with the new effective interaction labeled GXPF1 [5,6], which is based on effective two-body matrix elements with some replacement with the *G* matrix, were shown to reproduce well the systematic variation of the low-energy levels of the even-even nuclides in the vicinity of the $N = 32$ subshell closure. In addition, the *E*2 transition probabilities to the first excited 2^+ states in the even-even Ti isotopes were deduced by Dinca *et al.* [7], who used intermediate-energy Coulomb excitation. The $B(E2; 0^+ \rightarrow 2_1^+)$ values for ^{50}Ti$_{28}$ and ^{54}Ti$_{32}$ are comparable, within errors, providing further support for an $N = 32$ subshell closure for the Ti isotopes.

What is expected beyond $N = 32$, however, is still a matter of debate. The shell-model results obtained with GXPF1 suggested that the monopole shift of the $\nu f_{5/2}$ orbital is signficant enough to drive the state well above the $\nu p_{1/2}$ state with decreasing occupancy of the $\pi f_{7/2}$ orbital, producing a shell closure at $N = 34$ for both $_{22}$Ti and $_{20}$Ca [5]. No evidence was found for added stability at low energy in ^{56}Ti$_{34}$, where the first excited 2^+ state observed at 1129 keV [8,9] was nearly 400 keV below the predictions based on the GXPF1 interaction. Furthermore, the low-energy yrast structure of ^{56}Ti [10] derived from prompt γ-ray spectroscopy following deep-inelastic heavy-ion collisions is not suggestive of a large energy gap at $N = 34$ as predicted by the shell-model results obtained with GXPF1.

A strong proton-neutron monopole interaction may also be expected between the $\pi f_{7/2}$ and $\nu g_{9/2}$ orbitals [11]. The regular decrease in the excitation energy of the first 2^+ state in the even-even $_{26}$Fe [12] and $_{24}$Cr [13] isotopes near $N = 40$ has been attributed to the deformation-driving $\nu g_{9/2}$ orbital approaching the Fermi surface in these neutron-rich isotopes. Indeed, in ^{59}Cr$_{35}$ (discussed below), there is evidence for a low-energy $9/2^+$ isomeric state that has been proposed as an oblate-deformed Nilsson orbital originating from the spherical $\nu g_{9/2}$ orbital [14]. Therefore we have extended our previous studies of the β-decay of neutron-rich $_{22}$Ti [15] and $_{23}$V [16] isotopes to include ^{57}Ti and ^{59}V to further investigate the dynamic nature of the neutron *pfg* orbitals with filling of the $\pi f_{7/2}$ orbital.

Scant data are available in the literature regarding the β-decay properties of either ^{57}Ti or ^{59}V. Three previous measurements of the β-decay half-life of ^{57}Ti have been reported: Dörfler *et al.* [17] quote a value of 56 ± 20 ms; Sorlin *et al.* [18], 67 ± 25 ms; and Ameil *et al.* [19], 180 ± 30 ms. No information is available on excited states in the daughter ^{57}V; however, the β-decay of the ^{57}V has been well characterized [16]. The β-decay of ^{59}V was studied previously by Sorlin *et al.* [18] and, in addition to deducing a decay half-life of 75 ± 7 ms, they observed two β-delayed γ rays with energies of 102 and 208 keV. These same two γ rays, as well as a third with energy 193 keV, were assigned to the decay of a microsecond isomer in ^{59}Cr [20]. Although Grzywacz *et al.* [20] originally identified the 208-keV transition as the isomeric transition in ^{59}V, the subsequent β-decay work suggested that the 193-keV transition directly depopulates the isomeric $9/2^+$ state, which lies only 503 keV above the ^{59}Cr ground state. Freeman *et al.* [14] populated excited states in ^{59}Cr by a fusion-evaporation reaction and observed five γ rays; those at 102 and 208 keV, discussed above, and three more at 256, 518, and 813 keV. The last transition, with energy

813 keV, had the highest relative intensity and was assigned to the direct population of the proposed $9/2^+$ isomeric state. Coincidences across the isomer were not observed because of the long lifetime ($\sim$100 μs) of this state.

II. EXPERIMENTAL TECHNIQUE

The β-decay properties of ^{57}Ti and ^{59}V were studied through the use of the experimental facilities at the National Superconducting Cyclotron Laboratory (NSCL) at Michigan State University (MSU). A 140-MeV/nucleon ^{86}Kr^{34+} beam was produced by the coupled cyclotrons at the NSCL. The average beam current on target was 15 pnA. The ^{86}Kr primary beam was fragmented in a 376-mg/cm^2-thick Be target located at the object position of the A1900 fragment separator [21]. The secondary fragments of interest were selected in the A1900 by use of a 330-mg/cm^2 Al degrader and 1% momentum slits; both were located at the intermediate image of the device.

The fully stripped fragments were implanted in a double-sided Si microstrip detector (DSSD) with thickness 1470 μm that is part of the NSCL β-counting system [22]. Fragments were unambiguously identified by a combination of multiple energy-loss signals and time of flight. The fragment particle identification spectrum obtained with A1900 magnetic rigidities of $B\rho_1 = 4.239$ Tm and $B\rho_2 = 3.944$ Tm is shown in Fig. 1. A total of 1.92×10^5 ^{57}Ti ions and 5.40×10^5 ^{59}V ions were implanted into the DSSD.

Fragment-β correlations were established in software by the requirement of a high-energy implantation event in a single pixel of the DSSD followed by a low-energy β event in the same or any of the nearest eight neighboring pixels. The differences between the absolute time stamps of correlated β and implantation events were histogrammed to generate a decay curve. To suppress background, implantation events were rejected if they were not followed by a β event within 1 s or if they were followed by a second implantation within the same 1-s time period. The β-detection efficiency for both the ^{57}Ti and ^{59}V decays was $\sim$30%.
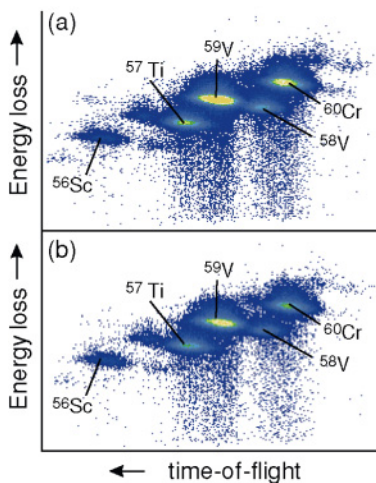

FIG. 1. (Color online) (a) Particle identification spectrum and (b) fragment-β correlated particle identification spectrum.
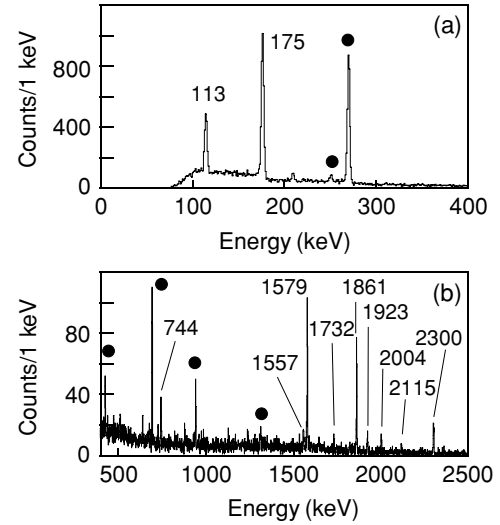

FIG. 2. β-delayed γ-ray spectrum from the decay of ^{57}Ti in the ranges (a) 0–0.4 MeV and (b) 0.4–2.5 MeV for events occurring within 1 s of an implanted ^{57}Ti ion. The filled circles indicate peaks corresponding to transitions previously assigned to the daughter ^{57}V decay.

Delayed γ rays were detected by 12 Ge detectors from the MSU segmented germanium array [23] arranged around the β-counting system, giving a total peak detection efficiency of 5.3% at 1 MeV. The energy resolution for each of the Ge detectors was measured to be $\sim$3.5 keV for the 1.3-MeV γ-ray transition in ^{60}Co.

III. RESULTS

A. ^{57}Ti

The β-delayed γ-ray spectrum for ^{57}Ti in the range 0–2.5 MeV is given in Fig. 2. The spectrum includes all γ rays detected within 1 s of the implantation of a ^{57}Ti ion. Six γ rays, including two prominent ones located at 268 and 692 keV, are known from the daughter decay of ^{57}V [16]. The γ rays attributed to the decay of ^{57}Ti are listed in Table I. There were

TABLE I. Energies and absolute intensities of delayed γ rays assigned to the decay of ^{57}Ti. The initial and final states for those transitions placed in the ^{57}V level scheme are also indicated.

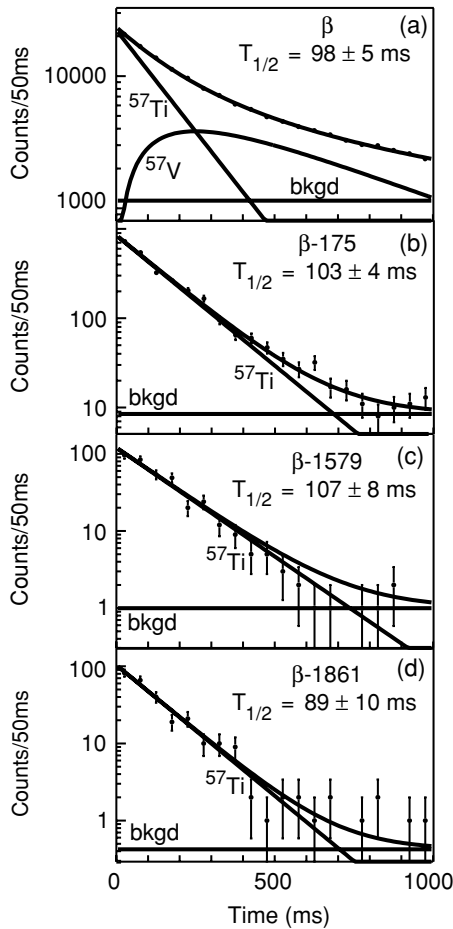| E_γ (keV)	I_γ^{abs} (%)	Initial state (keV)	Final state (keV)	Coincident γ rays (keV)
113.1 ± 0.4	14 ± 1	113	0	1579, 1861
174.8 ± 0.4	31 ± 2	175	0	1579, 1861
744.0 ± 0.4	2.3 ± 0.4	2476	1732	175, 1557, 1732
1557.3 ± 0.5	2.2 ± 0.5	1732	175	175
1579.4 ± 0.4	16 ± 2	1754	175	113, 175
1732.2 ± 0.6	1.2 ± 0.2	1732	0	744
1861.5 ± 0.4	14 ± 2	2036	175	113, 175
1922.9 ± 0.5	2.6 ± 0.5	2036	113	113
2003.7 ± 0.6	1.8 ± 0.5			
2114.6 ± 0.5	0.7 ± 0.3			
2300.4 ± 0.4	5.0 ± 0.5	2476	175	113, 175

FIG. 3. Decay curve for ^{57}Ti showing fragment-β correlations (a) in which the data were fit with an exponential parent decay, an exponential growth, and decay for the daughter ^{57}V and a linear background. Decay curves with an additional requirement of a coincident γ ray with energies of (b) 175 keV, (c) 1579 keV, and (d) 1861 keV were fitted with an exponential decay and linear background.

FIG. 4. Proposed ^{57}V level scheme populated following the decay of ^{57}Ti. The number in brackets following a γ-ray transition energy is the absolute γ-ray intensity. The Q value was deduced from data in Ref. [24]. Observed coincidences are represented as filled circles. Absolute β-decay intensities and apparent log ft values to each state in ^{57}V are given on the left-hand side of the figure.

results, a value of 98 ± 5 ms for the half-life of ^{57}Ti has been adopted.

The proposed low-energy level scheme of ^{57}V populated following the β-decay of ^{57}Ti is presented in Fig. 4. All of the proposed levels follow from $\gamma\gamma$ coincidence relationships. Based on the efficiency-corrected intensity ratios between the 113- and 175-keV peaks in the 1579- and 1861-keV γ-gated coincidence spectra (see Fig. 5), the 113- and 175-keV

no γ rays that could be associated with the low-energy levels of ^{56}V; therefore it does not appear that there is a significant delayed neutron branch to excited levels in ^{56}V.

The half-life of ^{57}Ti deduced from a fit of the fragment-β-decay curve presented in Fig. 3(a) is 98 ± 5 ms. The decay curve was fitted considering the exponential decay of the parent, exponential growth, and decay of the daughter ^{57}V, and a linear background term. The half-life of the daughter ^{57}V was taken to be 350 ms [16]. Fragment-β–γ-decay curves were also analyzed for each of the γ-ray transitions assigned to ^{57}Ti. Examples for the more intense γ rays with energies of 175, 1579, and 1861 keV are also shown in Fig. 3. The γ-gated decay curves were fitted with an exponential decay and a linear background component. The deduced half-life values were consistent, within errors, with the half-life determined from the fragment-β-decay curve, verifying their assignments to the decay of ^{57}Ti. Previous measurements of the ^{57}Ti half-life include values of 67 ± 25 ms [18], 180 ± 30 ms [19], and 56 ± 20 ms [17]. However, these measurements isolated ^{57}Ti in very small quantities. Based on the present half-life
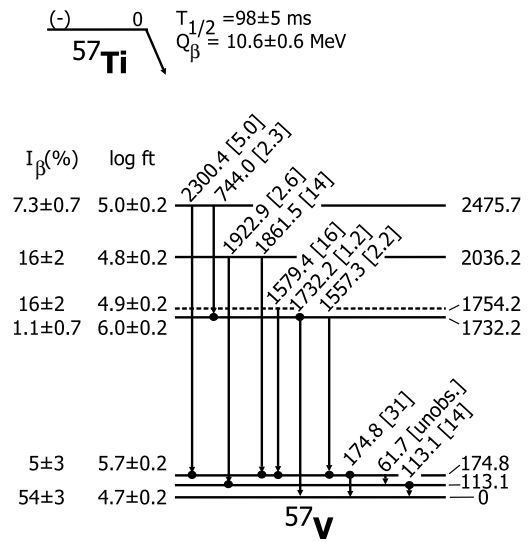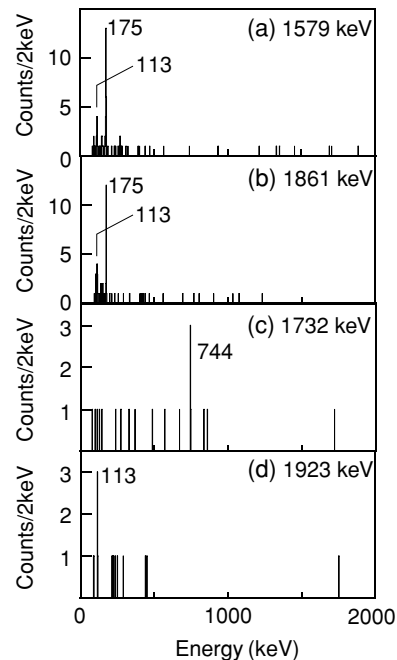

FIG. 5. $\gamma\gamma$ coincidence spectra for the (a) 1579-, (b) 1861-, (c) 1732-, and (d) 1923-keV transitions following ^{57}Ti β-decay.
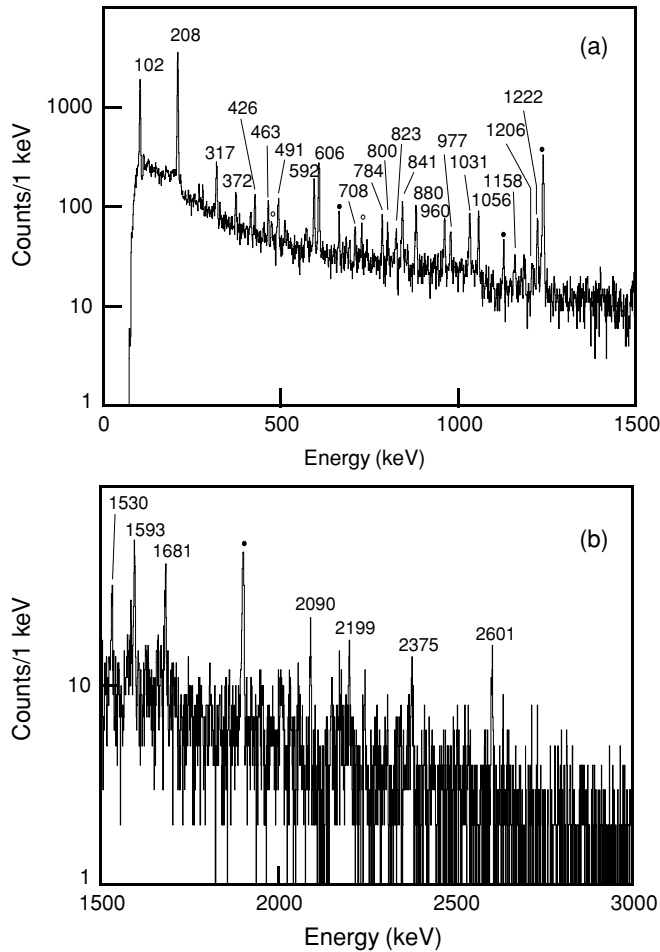
FIG. 6. ^{59}V β-delayed γ rays in the ranges (a) 0–1.5 MeV and (b) 1.5–3.0 MeV for events that occurred within 1 s of a ^{59}V implanted ion. The filled and open circles indicate peaks corresponding to transitions previously assigned to the daughter ^{59}Cr and granddaughter ^{59}Mn decays, respectively.

ratios, as well as the deduced apparent log *ft* values, are given in Fig. 4. The experimental Q_β value of 10.6 ± 0.6 MeV was deduced from data in Ref. [24]. The large Q-value window and limitations on the detection of γ rays with absolute intensities below 1% permit only limited interpretations by use of the apparent log *ft* values. However, a significant portion of the apparent β feeding directly populates the ground state of ^{57}V. Further details regarding the feeding patterns to levels in ^{57}V are left for the discussion.

B. ^{59}V

The β-delayed γ-ray spectrum in the energy range of 0–3 MeV for those events observed within 1 s of the implantation of a ^{59}V ion into the DSSD is given in Fig. 6. Numerous γ-ray transitions are observed in this spectrum, and those assigned to the decay of ^{59}V are listed in Table II. Other γ rays present

TABLE II. Energies and absolute intensities of delayed γ rays assigned to the decay of ^{59}V. The initial and final states for those transitions placed in the ^{59}Cr level scheme are also indicated.

Energy (keV)	I_γ^{abs} (%)	Initial state (keV)	Final state (keV)	Coincident γ rays (keV)
102.0 ± 0.4	21 ± 2	310	208	208, 426, 491, 606, 977, 1031, 1056, 1530
207.8 ± 0.4	41 ± 3	208	0	102, 317, 372, 491, 592, 606, 708, 841, 977, 1031, 1056, 1222
317.3 ± 0.4	3.0 ± 0.4	525	208	208, 841
371.7 ± 0.5	1.6 ± 0.3			208
425.5 ± 0.4	1.7 ± 0.3	1341	915	102, 208, 606, 1530
463.1 ± 0.4	1.7 ± 0.2			208, 823
490.8 ± 0.5	2.3 ± 0.4	800	310	102, 208
592.4 ± 0.4	4.2 ± 0.3	800	208	208
606.0 ± 0.4	6.4 ± 0.4	915	310	102, 208, 426
707.6 ± 0.5	1.1 ± 0.3	915	208	208
784.1 ± 0.4	1.8 ± 0.3			102, 208
799.9 ± 0.5	1.1 ± 0.3	800	0	
823.2 ± 0.6	1.1 ± 0.3			208, 463, 1222
841.4 ± 0.4	2.7 ± 0.3	1366	525	208, 317
879.9 ± 0.5^a	3.0 ± 0.4			1056
959.9 ± 0.4	2.2 ± 0.3			208
977.2 ± 0.5	1.4 ± 0.2	2509	1532	102, 208
1030.8 ± 0.4	2.4 ± 0.3	1341	310	102, 208
1056.0 ± 0.4^a	2.5 ± 0.3	1366	310	102, 208, 880
1157.8 ± 0.5	0.8 ± 0.2	1366	208	
1206.5 ± 0.6	0.6 ± 0.2			
1222.1 ± 0.4	2.5 ± 0.3	1532	310	102, 208
1529.6 ± 0.5	1.0 ± 0.3			102, 208
1593.4 ± 0.5	2.2 ± 0.4	2509	915	
1680.9 ± 0.5	1.9 ± 0.3			
2089.6 ± 0.5	0.9 ± 0.2			
2198.7 ± 0.5	0.5 ± 0.2	2509	310	
2375.0 ± 0.6	0.8 ± 0.2			
2601.3 ± 0.6	1.2 ± 0.2			

^{a}Possible β-delayed neutron branch to excited levels in ^{58}Cr. See text for details.

transitions were placed in parallel. Inspection of the 1923-keV coincidence gated spectrum suggests that this transition should be placed as directly feeding the 113-keV state. The absence of peaks at both 113 or 175 keV in the 1732-keV gated coincidence spectrum established the 1732-keV level. There is a coincidence observed between the 744- and 1732-keV lines, and the former transition has been placed as depopulating a level at 2476 keV. The presence of both the 113- and 175-keV transitions in the coincidence spectra for the 1579- and 1861-keV γ rays suggests that there is an unobserved 62-keV γ ray depopulating the 175-keV state. Such a low-energy transition would have been below the hardware thresholds set for the Ge detectors. The order of the 62- and 113-keV transitions is determined by the 1923-keV γ ray, which depopulates the level at 2036 keV and is in coincidence with only the 113-keV γ ray.

The apparent β feedings in ^{57}V were determined from differences in absolute γ-ray intensities for transitions into and out of each level. The ground-state feeding was deduced by use of the additional knowledge of the total number of ^{57}Ti parent nuclei implanted into the DSSD. The β-branching
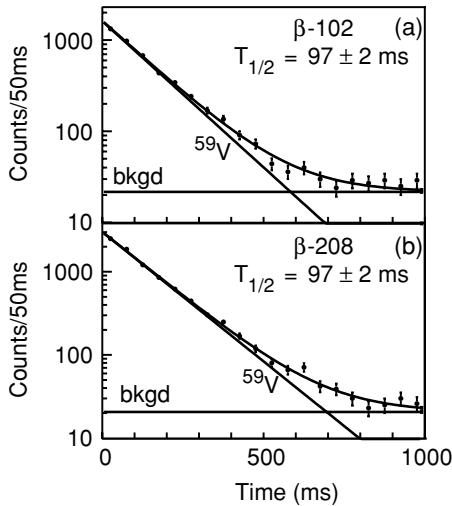
FIG. 7. Decay curves for ^{59}V showing fragment-β correlations with an additional requirement of a coincident γ ray with an energy of (a) 102 keV and (b) 208 keV. The decay curves were fitted with an exponential function with linear background.

FIG. 8. Proposed ^{59}Cr level scheme populated following the decay of ^{59}V. The number in brackets following a γ-ray transition energy is the absolute γ-ray intensity. The Q value was deduced from data in Ref. [24]. Observed coincidences are represented as filled circles.

included those from the decay of the ^{59}V daughter, which are discussed in more detail below, and of the ^{59}Mn granddaughter, which were readily identified from the decay curves gated on individual γ-ray transitions. Of the γ rays listed in Table II, those with energies of 102 and 208 keV were observed in previous studies of the decay of excited states in ^{59}Cr [14,18,20].

In Fig. 7 are presented the fragment-β-decay curves gated on the 102- and 208-keV γ-ray transitions assigned to ^{59}V decay. A half-life of 97 ± 2 ms was deduced for the ground-state decay of ^{59}V. Other decay curves gated on delayed transitions assigned to the decay of ^{59}V revealed half-lives consistent within the statistical error of this result.

The proposed level scheme for ^{59}Cr populated through the β-decay of ^{59}V is introduced in Fig. 8. The γ rays with energies of 102 and 208 keV were identified and placed into a level scheme previously [18]. The placement of these two γ rays in series, with the lowest excited state at an energy of 208 keV, was confirmed by the $\gamma\gamma$ coincidence spectra obtained in this experiment and shown in Fig. 9. Such a placement refutes the findings presented in Ref. [14], in which the 102- and 208-keV transitions are reversed in the level scheme. In particular, the coincidence spectra gated on the 317-, 592-, and 708-keV transitions show only the 208-keV transition, and not a transition with an energy of 102 keV. Because the 208- and 102-keV transitions are in cascade, the 208-keV γ ray must directly populate the ^{59}Cr ground state. Of the other γ rays assigned to the decay of ^{59}V, most feed directly the levels at either 208 or 310 keV, and these coincidence relationships helped define the proposed level structure above 500 keV. The proposed state at 525 keV is shown as a tentative placement because the order of the 371- and 841-keV transitions could not be determined explicitly. A similar situation exists for the 1532-keV state, which is based on the 208–1222 coincidence, although the ordering of the
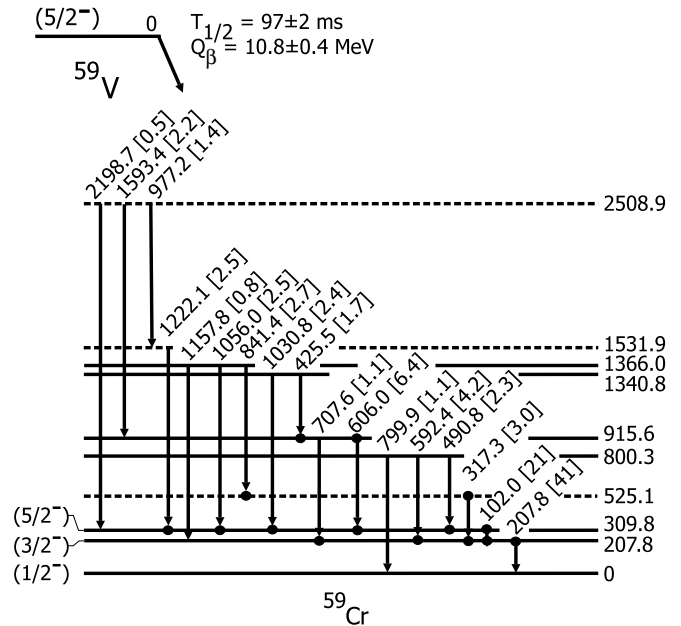
977- and 1222-keV γ rays could not be resolved from the available data. The tentative level at 2509 keV is the only proposed level not based on coincidences; energy-sum relationships were used to place the 977-, 1593-, and 2199-keV γ rays as depopulating the proposed 2509-keV state.

The log ft values and β-decay branching ratios were not deduced because there are still a number of unassigned γ-ray transitions. However, it should be noted that, based on the total number of β-decays observed and the summed intensities of γ-ray transitions that directly populate the ground state, there is apparent direct β feeding to the ground state of ^{59}Cr.

Sorlin *et al.* [18] had previously proposed spin and parity assignments of $1/2^-$, $3/2^-$, and $5/2^-$ for the ground and first two excited states of ^{59}Cr, respectively. The spin and parity of the 310-keV level are based on the $M2$ character of the 193-keV isomeric γ ray that depopulates the proposed $9/2^+$ level at 503 keV [20]. The tentative $1/2^-$ and $3/2^-$ spin and parity assignments for the ground and first excited states are supported in this measurement. If the spin assignments were reversed, the 102- keV transition would have $E2$ multipolarity, and a lifetime of the order of a few microseconds would be expected based on Weisskopf estimates. However, no evidence of a long lifetime (greater than 200 ns) for the 102-keV γ-ray transition was found.

It should be noted that a small β-delayed neutron branch cannot be ruled out for the decay of ^{59}V. The 880- and 1056-keV γ-ray transitions assigned to levels in ^{58}Cr [16] have also been observed in the delayed γ-ray spectrum for ^{59}V as displayed in Fig. 6. A 1056-keV γ ray was observed in coincidence with the 102- and 208-keV γ rays assigned to the
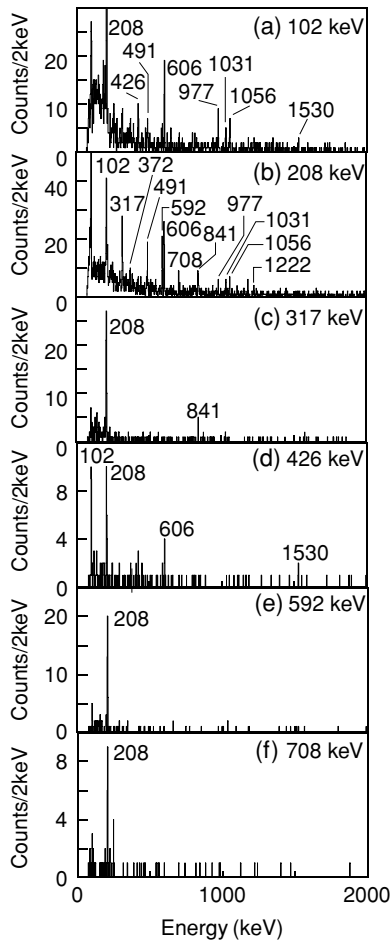
FIG. 9. $\gamma\gamma$ coincidence spectra following ^{59}V β decay for the (a) 102-, (b) 208-, (c) 317-, (d) 426-, (e) 592-, and (f) 708-keV transitions.

decay of ^{59}V. Based on the absolute intensity of the 880-keV γ ray, which is not observed in coincidence with γ rays assigned to ^{59}V, the β-delayed neutron branch to levels in ^{58}V that directly feed the 2_1^+ state is deduced to be $\sim$3%; this should be considered a lower limit.

C. ^{59}Cr

The first adopted half-life of ^{59}Cr, 740 ± 240 ms [25,26], was obtained from an average of the γ-gated half-lives of 1.0 ± 0.4 s and 0.6 ± 0.3 s for the 1238- and 112-keV γ rays, respectively, weighted by their relative intensities. A subsequent measurement of the β-decay of ^{59}Cr by Dörfler *et al.* [17] resulted in a half-life value of 460 ± 46 ms. We have deduced a new half-life of ^{59}Cr based on a decay curve gated on the 1238-keV γ ray assigned to the granddaughter ^{59}Mn, as shown in Fig. 10(a). The curve in Fig. 10(a) was fitted considering the exponential growth and decay of ^{59}Cr as well as a linear background. A half-life of the ^{59}V parent was taken to be the present value of 97 ms. The deduced half-life of ^{59}Cr was 1050 ± 90 ms.

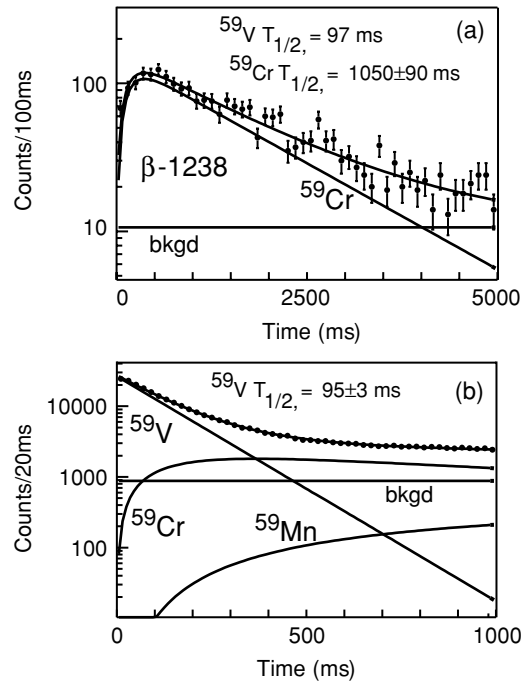This new value of the ^{59}Cr half-life was used to fit the daughter contribution to the ^{59}V fragment-β-decay curve,

FIG. 10. (a) Decay curve showing fragment-β correlations in the decay of ^{59}V with an additional requirement of a coincident γ ray with an energy of 1238 keV. The function used to fit the decay curve data included the exponential growth and decay of the daughter ^{59}Cr with a linear background. The half-life for the parent ^{59}V was fixed at 97 ms. The $\beta\gamma$ correlation time was extended to 5 s for these data to fully account for the longer half-life of the ^{59}Cr daughter. (b) Decay curve showing fragment-β correlations for events occurring within 1 s after a ^{59}V implanted ion. The decay curve was fitted with an exponential decay of the parent, growth, and decay of the daughter and granddaughter and a linear background term. The half-life of the daughter ^{59}Cr was fixed at 1050 ms.

given in Fig. 10(b). Here, the fit function included exponential decay of the ^{59}V parent, exponential growth and decay of the ^{59}Cr daughter with a fixed half-life of 1050 ms, and a linear background. A half-life value of 95 ± 3 ms was deduced for ^{59}V, in agreement with the adopted half-life of 97 ± 2 ms based on fits of the fragment-$\beta-\gamma$-decay curves in Fig. 7.

The new half-life value of 1050 ± 90 ms for the ^{59}Cr β-decay agrees, within errors, with the first adopted half-life of ^{59}Cr, which was deduced from the decay characteristics of daughter γ rays [25,26]. Disagreement with the half-life value quoted by Dörfler *et al.* [17] might be attributed to the limited $\beta\gamma$ statistics obtained in this earlier measurement.

A proposed level scheme for ^{59}Mn populated following the β-decay of ^{59}Cr is given in Fig. 11. $\gamma\gamma$ coincidence spectra used for γ-ray placement in ^{59}Mn are presented in Fig. 12. The 662- and 1238-keV γ rays were found to be in coincidence. A mutual coincidence was not observed for the 112- and 1238-keV transitions, and both are placed as directly feeding the ^{59}Mn ground state.
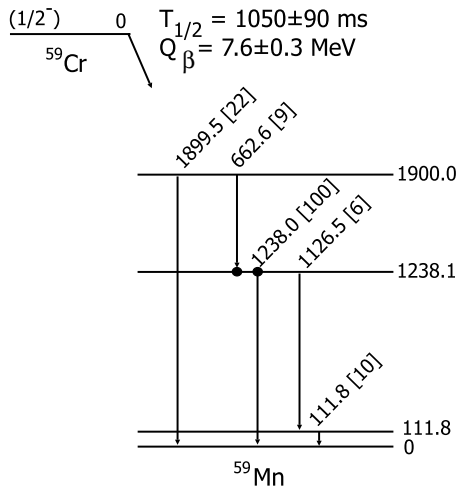
FIG. 11. Proposed ^{59}Mn level scheme from the decay of ^{59}Cr. The number in brackets following a γ-ray transition energy is the relative γ-ray intensity. The Q value was deduced from data in Ref. [24]. Observed coincidences are represented as filled circles.

IV. DISCUSSION

Calculations of the β-decay of ^{57}Ti to low-energy levels in ^{57}V were carried out with the pf shell-model interaction GXPF1 [5,6] and the codes OXBASH [27] and CMICHSM [28]. The GXPF1 interaction is known to overpredict the energy gap between the neutron $f_{5/2}$ and $p_{1/2}$ orbitals at $N = 34$ [8], and a new interaction GXPF1A has been introduced that involves modifications to the $T = 1$ two-body matrix elements as a means for better reproducing the yrast energy spectrum of ^{56}Ti [7,10]. The β-decay properties of neutron-rich $_{22}$Ti [15] and $_{23}$V [16] were successfully reproduced with the GXPF1 interaction, and therefore we elected again to apply the GXPF1 interaction for the shell-model calculations reported here. The
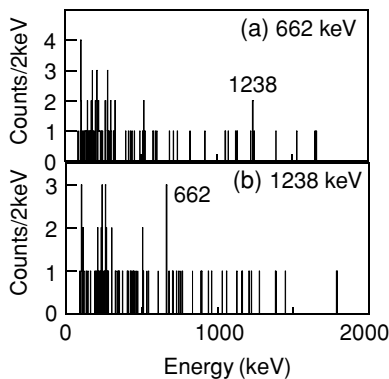

FIG. 12. $\gamma\gamma$ coincidence spectra for the (a) 662- and (b) 1238-keV transitions assigned to the decay of ^{59}Cr. The 1238- and 662-keV transitions were observed in mutual coincidence. A coincidence between the 1238- and 112-keV transitions, if present, should be observable in the 1238-keV gated spectrum based on the intensity of the 662-keV peak. Intensities were too weak to determine coincidences between 662- and either of the 112- or 1126-keV transitions.
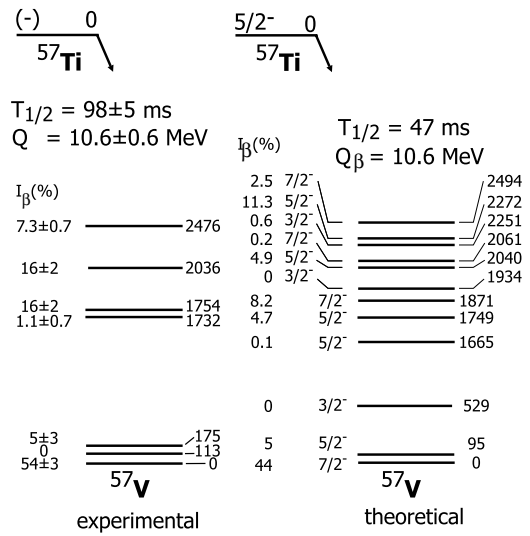

FIG. 13. The experimental decay scheme for levels in ^{57}V populated following the β-decay of ^{57}Ti and shell-model results carried out in the full pf space with the interaction GXPF1. The shell-model results assume a ^{57}Ti ground state with a spin and parity of $5/2^-$.

goal of selecting the GXPF1 interaction was to further identify potential deficiencies in the GXFP1 interaction related to the β-decay matrix elements.

The ground-state spin and parity of ^{57}Ti are expected to be $5/2^-$, based on the shell-model results obtained with the GXPF1 interaction. Such a spin and parity assignment for the ground state is consistent with the odd neutron in ^{57}Ti occupying the $\nu f_{5/2}$ orbital. Previous results with the GXPF1 interaction have shown that, for ^{55}Ti, the ground-state spin and parity are expected to be $1/2^-$, suggesting that the effective single-particle energy of the $\nu p_{1/2}$ orbital is lower than that for the $\nu f_{5/2}$ orbital. The first excited state in ^{57}Ti is calculated to lie at an energy of 422 keV, with spin and parity $1/2^-$. The calculations of the β-decay properties of ^{57}Ti have therefore been carried out assuming $5/2^-$ spin and parity for the ground state.

The calculated β-decay of ^{57}Ti to levels in ^{57}V is presented in Fig. 13. Considering that the lower detection limit for absolute intensities in the ^{57}Ti β-decay was $\sim 0.7\%$, the experimental and calculated β-decay properties agree quite well. Direct β feeding to the ^{57}V ground state is estimated at 44%, which compares favorably with the deduced ground-state β branch of $54\% \pm 3\%$. The shell-model results also predict a significant amount of β-decay feeding to four states above 1500 keV in ^{57}V, which correspond well with the observed apparent β branchings.

Some correspondence between the proposed low-energy-level structure of ^{57}V fed in β-decay and that predicted by the shell-model calculations is apparent. There is nearly a 1.5-MeV gap between the triplet of levels observed experimentally near the ^{57}V ground state and the next proposed level at 1732 keV. The shell-model results obtained with GXPF1 include a shell closure at $N = 34$ [5], leading to the low-level density below 1.7 MeV in ^{57}V, as seen in Fig. 13.

The low-energy triplet most likely corresponds to the lowest three levels with spins and parities of $7/2^-$, $5/2^-$, and $3/2^-$ resulting from the shell-model calculations with the GXPF1 interaction. The spread of the lowest three calculated levels in ^{57}V, compared with the new experimental results, is within the limits of accuracy of the GXPF1 interaction, which we obtained by fitting 699 levels in 87 pf nuclei with a root-mean-square deviation of 168 keV [6]. A tentative spin and parity assignment of $3/2^-$ for the ground state of ^{57}V was initially proposed by Sorlin *et al.* [29], based on the characteristics of the β-decay into levels of ^{57}Cr compared with quasiparticle random-phase approximation calculations. Later, the ^{57}V $\rightarrow$ ^{57}Cr ground-state branch was remeasured and resulted in a value of 21% [16]. A comparison of the ^{57}V β-decay characteristics with the results of GXPF1 shell-model calculations favored a spin and parity of either $5/2^-$ or $7/2^-$ for the ground state of ^{57}V. The significant direct β-decay branch to the ^{57}V ground state would favor a $7/2^-$ spin and parity assignment based on the shell-model calculations. Such a spin and parity assignment to the ground state of ^{57}V would suggest a less deformed (slightly oblate) structure based on the potential-energy surfaces calculated for the odd-A V isotopes in Ref. [18].

The low-energy structure of ^{59}Cr proposed here differs from that in Ref. [14] only in the order of the γ-ray cascade, including the 208- and 102-keV transitions. The tentative spin and parity assignment of $5/2^-$ for the ground state of the ^{59}V parent is taken from Sorlin *et al.* [18]. The low-energy-level scheme from the shell-model calculations in the full pf shell with the GXPF1 interaction is given by Freeman *et al.* [14] and shows only seven negative-parity levels below 1.6 MeV. The level structure of ^{59}Cr proposed in Fig. 8 has eight excited levels below 1.6 MeV. Although not all are directly populated in β-decay, based on the tentative $5/2^-$ spin and parity assignment to the ^{59}V β-decaying state and the average number of cascade γ rays of ≈ 2, all of these excited levels are most likely of negative parity with spins $\leqslant 9/2$. No evidence for a 813-keV γ ray as observed by Freeman *et al.* and placed as directly populating the proposed $9/2^+$ level in ^{59}Cr at 503 keV was observed. However, this is not surprising because direct β feeding to such a state in ^{59}Cr would be highly forbidden. Furthermore, no evidence for a transition at 518 keV, which was tentatively placed as depopulating a proposed $7/2^-$ state at 828 keV in ^{59}Cr [14], was observed. The absence of a crossover $E2$ γ-ray transition between the proposed $5/2^-$ state at 310 keV and the ^{59}Cr ground state is corroborated by the shell-model calculations results obtained with the GXPF1 interaction.

The presence of the $9/2^+$ level at low energy in ^{59}Cr is suggestive of deformation. Freeman *et al.* [14] proposed moderate oblate deformation ($\beta_2 \sim -0.2$) based on comparisons of the low-energy structure with the Nilsson model. Such an interpretation is not altered by the reordering of the 208- and 102-keV γ-ray transitions. Indeed, as Freeman *et al.* note, low-energy states with spin and parities $3/2^-$ and $5/2^-$ can be readily generated by single-neutron excitations into states with spherical $\nu f_{5/2}$ parentage if oblate deformation is considered.

V. SUMMARY

Details regarding the β-decay properties of ^{57}Ti and ^{59}V were reported. New half-life values of 98 ± 5 ms for ^{57}Ti and 97 ± 2 ms for ^{59}V were deduced from β-decay curves gated on known γ-ray transitions. A new half-life value of 1050 ± 90 ms was also deduced for the daughter ^{59}Cr β-decay, again based on fitting of the γ-gated β-decay curves. The low-energy-level structures of the daughter nuclides ^{57}V and ^{59}Cr were compared with shell-model results calculated in the full pf shell by use of the GXPF1 interaction. The three lowest-energy states in ^{57}V reside within 200 keV of the ground state, whereas the next group of excited states observed experimentally lie more than 1.5 MeV above the ^{57}V ground state. Some correspondence with the shell-model results were revealed, especially between the energies and β branchings to the three lowest-energy states in ^{57}V. The low-energy-level structure observed for ^{59}Cr appears more complicated than that predicted by shell-model calculations. The $9/2^+$ spin and parity assignment previously made to the 503-keV level suggests that the $\nu g_{9/2}$ shell-model orbital has influence, even at low energy, in the neutron-rich $_{24}$Cr nuclides. Both ^{57}V and ^{59}Cr show evidence of oblate deformation near the ground state.

[1] J. I. Prisciandaro, P. F. Mantica, B. A. Brown, D. W. Anthony, M. W. Cooper, A. Garcia, D. E. Groh, A. Komives, W. Kumarasiri, P. A. Lofy, A. M. Oros-Peusquens, S. L. Tabor, and W. Wiedeking, Phys. Lett. **B510**, 17 (2001).

[2] D. E. Appelbe, C. J. Barton, M. H. Muikku, J. Simpson, D. D. Warner, C. W. Beausang, M. A. Caprio, J. R. Cooper, J. R. Novak, N. V. Zamfir, R. A. E. Austin, J. A. Cameron, C. Malcolmson, J. C. Waddington, and F. R. Xu, Phys. Rev. C **67**, 034309 (2003).

[3] R. V. F. Janssens, B. Fornal, P. F. Mantica, B. A. Brown, R. Broda, P. Bhattacharyya, M. P. Carpenter, M. Cinausero, P. J. Daly, A. D. Davies, T. Glasmacher, Z. W. Grabowski, D. E. Groh, M. Honma, F. G. Kondev, W. Krolas, T. Lauritsen, S. N. Liddick, S. Lunardi, N. Marginean, T. Mizusaki, D. J. Morrissey, A. C. Morton, W. F. Mueller, T. Otsuka, T. Pawlat, D. Seweryniak, H. Schatz, A. Stolz, S. L. Tabor, C. A. Ur, G. Viesti, I. Wiedenhoever, and J. Wrzesinski, Phys. Lett. **B546**, 55 (2002).

[4] A. Huck, G. Klotz, A. Knipper, C. Miehe, C. Richard-Serre, G. Walter, A. Poves, H. L. Ravn, and G. Marguier, Phys. Rev. C **31**, 2226 (1985).

[5] M. Honma, T. Otsuka, B. A. Brown, and T. Mizusaki, Phys. Rev. C **65**, 061301(R) (2002).

[6] M. Honma, T. Otsuka, B. A. Brown, and T. Mizusaki, Phys. Rev. C **69**, 034335 (2004).

[7] D.-C. Dinca, R. V. F. Janssens, A. Gade, D. Bazin, R. Broda, B. A. Brown, C. M. Campbell, M. P. Carpenter, P. Chowdhury, J. M. Cook, A. N. Deacon, B. Fornal, S. J. Freeman, T. Glasmacher, M. Honma, F. G. Kondev, J.-L. Lecouey, S. N. Liddick, P. F. Mantica, W. F. Mueller, H. Olliver, T. Otsuka, J. R. Terry, B. A. Tomlin, and K. Yoneda, Phys. Rev. C **71**, 041302(R) (2005).

[8] S. N. Liddick, P. F. Mantica, R. V. F. Janssens, R. Broda, B. A. Brown, M. P. Carpenter, B. Fornal, M. Honma, T. Mizusaki, A. C. Morton, W. F. Mueller, T. Otsuka, J. Pavan, A. Stolz, S. L. Tabor, B. E. Tomlin, and M. Wiedeking, Phys. Rev. Lett. **92**, 072502 (2004).

[9] S. N. Liddick, P. F. Mantica, R. Broda, B. A. Brown, M. P. Carpenter, A. D. Davies, B. Fornal, T. Glasmacher, D. E. Groh, M. Honma, M. Horoi, R. V. F. Janssens, T. Mizusaki, D. J. Morrissey, A. C. Morton, W. F. Mueller, T. Otsuka, J. Pavan, H. Schatz, A. Stolz, S. L. Tabor, B. E. Tomlin, and M. Wiedeking, Phys. Rev. C **70**, 064303 (2004).

[10] B. Fornal, S. Zhu, R. V. F. Janssens, M. Honma, R. Broda, P. F. Mantica, B. A. Brown, M. P. Carpenter, P. J. Daly, S. J. Freeman, Z. W. Grabowski, N. J. Hammond, F. G. Kondev, W. Królas, T. Lauritsen, S. N. Liddick, C. J. Lister, E. F. Moore, T. Otsuka, T. Pawlat, D. Seweryniak, B. E. Tomlin, and J. Wrzesinski, Phys. Rev. C **70**, 064304 (2004).

[11] A. M. Oros-Peusquens and P. F. Mantica, Nucl. Phys. **A669**, 81 (2000).

[12] M. Hannawald, T. Kautzsch, A. Wöhr, W. B. Walters, K. L. Kratz, V. N. Fedoseyev, V. I. Mishin, W. Bohmer, B. Pfeiffer, V. Sebastian, Y. Jading, U. Köster, J. Lettry, H. L. Ravn (ISOLDE Collaboration), Phys. Rev. Lett. **82**, 1391 (1999).

[13] O. Sorlin, C. Donzaud, F. Nowacki, J. C. Angelique, F. Azaiez, C. Bourgeois, V. Chiste, Z. Dlouhy, S. Grevy, D. Guillemaud-Mueller, F. Ibrahim, K.-L. Kratz, M. Lewitowicz, S. M. Lukyanov, J. Mrazek, Yu.-E. Penionzhkevich, F. de Oliveira Santos, B. Pfeiffer, F. Pougheon, A. Poves, M. G. Saint-Laurent, and M. Stanoiu, Eur. Phys. J. A **16**, 55 (2003).

[14] S. J. Freeman, R. V. F. Janssens, B. A. Brown, M. P. Carpenter, S. M. Fischer, N. J. Hammond, M. Honma, T. Lauritsen, C. J. Lister, T. L. Khoo, G. Mukherjee, D. Seweryniak, J. F. Smith, B. J. Varley, M. Whitehead, and S. Zhu, Phys. Rev. C **69**, 064301 (2004).

[15] P. F. Mantica, B. A. Brown, A. D. Davies, T. Glasmacher, D. E. Groh, M. Horoi, S. N. Liddick, D. J. Morrissey, A. C. Morton, W. F. Mueller, H. Schatz, A. Stolz, and S. L. Tabor, Phys. Rev. C **68**, 044311 (2003).

[16] P. F. Mantica, A. C. Morton, B. A. Brown, A. D. Davies, T. Glasmacher, D. E. Groh, S. N. Liddick, D. J. Morrissey, W. F. Mueller, H. Schatz, A. Stolz, S. L. Tabor, M. Honma, M. Horoi, and T. Otsuka, Phys. Rev. C **67**, 014311 (2003).

[17] T. Dörfler, W.-D. Schmidt-Ott, T. Hild, T. Mehren, W. Böhmer, P. Möller, B. Pfeiffer, T. Rauscher, K.-L. Kratz, O. Sorlin, V. Borrel, S. Grévy, D. Guillemaud-Mueller, A. C. Mueller, F. Pougheon, R. Anne, M. Lewitowicz, A. Ostrowsky, M. Robinson, and M. G. Saint-Laurent, Phys. Rev. C **54**, 2894 (1996).

[18] O. Sorlin, C. Donzaud, L. Alexsson, M. Belleguic, R. Béraud, C. Borcea, G. Canchel, E. Chabanat, J. M. Daugas, A. Emsallem, D. Guillemaud-Mueller, K.-L. Kratz, S. Leenhardt, M. Lewitowicz, C. Longour, M. J. Lopez, F. de Oliveira Santos, L. Petizon, B. Pfeiffer, F. Pougheon, M. G. Saint-Laurent, and J. Sauvestre, Nucl. Phys. **A660**, 3 (1999).

[19] F. Ameil, M. Bernas, P. Armbruster, S. Czajkowski, Ph. Dessagne, H. Geissel, E. Hanelt, C. Kozhuharov, C. Miehe, C. Donzaud, A. Grese, A. Heinz, Z. Janas, M. de Jong, W. Schwab, S. Steinhäuser, Eur. Phys. J. A **1**, 275 (1998).

[20] R. Grzywacz, R. Béraud, C. Borcea, A. Emsallem, M. Glogowski, H. Grawe, D. Guillemaud-Mueller, M. Hjorth-Jensen, M. Houry, M. Lewitowicz, A. C. Mueller, A. Nowak, A. Plochocki, M. Pfützner, K. Rykaczewski, M. G. Saint-Laurent, J. E. Sauvestre, M. Schaefer, O. Sorlin, J. Szerypo, W. Trinder, S. Viteritti, and J. Winfield, Phys. Rev. Lett. **81**, 766 (1998).

[21] D. J. Morrissey, B. M. Sherrill, M. Steiner, A. Stolz, and I. Wiedenhöver, Nucl. Instrum. Methods Phys. Res. B **204**, 90 (2003).

[22] J. I. Prisciandaro, A. C. Morton, and P. F. Mantica, Nucl. Instrum. Methods Phys. Res. A **505**, 140 (2003).

[23] W. F. Mueller, J. A. Church, T. Glasmacher, D. Gutknecht, G. Hackman, P. G. Hansen, Z. Hu, K. L. Miller, P. Quirin, Nucl. Instrum. Methods Phys. Res. A **466**, 492 (2001).

[24] G. Audi, A. H. Wapstra, and C. Thibault, Nucl. Phys. **A729**, 337 (2003).

[25] U. Bosch, W.-D. Schmidt-Ott, P. Tidemand-Petersson, E. Runte, W. Hillebrandt, M. Lechle, F.-K. Thielemann, R. Kirchner, O. Klepper, E. Roeckl, K. Rykaczewski, D. Schardt, N. Kaffrell, M. Bernas, Ph. Dessagne, and W. Kurcewicz, Phys. Lett. **B164**, 22 (1985).

[26] U. Bosch, W.-D. Schmidt-Ott, E. Runte, P. Tidemand-Petersson, P. Koschel, F. Meissner, R. Kirchner, O. Klepper, E. Roeckl, K. Rykaczewski, and D. Schardt, Nucl. Phys. **A477**, 89 (1988).

[27] B. A. Brown, A. Etchegoyen, and W. D. M. Rae, The computer code OXBASH, MSU-NSCL Report No. 524, 1998.

[28] M. Horoi, B. A. Brown, and V. Zelevinsky, Phys. Rev. C **67**, 034303 (2003).

[29] O. Sorlin, V. Borrel, S. Grévy, D. Guillemaud-Mueller, A. C. Mueller, F. Pougheon, W. Böhmer, K.-L. Kratz, T. Mehren, P. Möller, B. Pfeiffer, T. Rauscher, M. G. Saint-Laurent, R. Anne, M. Lewitowicz, A. Ostrowski, T. Dörfler, and W.-D. Schmidt-Ott, Nucl. Phys. **A632**, 205 (1998).